Analytical and Experimental Demonstration of an Alternate Mixing Performance Metric for High-Speed Fuel Mixing Studies

Cody R. Ground*, Karen F. Cabell†, Tomasz G. Drozda‡
Hypersonic Airbreathing Propulsion Branch, NASA Langley Research Center, Hampton, VA, 23681

To experimentally assess the fuel/air mixing performance of high-speed fuel injectors, one-dimensional metrics that quantify the degree of mixing completeness downstream of the fuel injection location are required. The most accurate assessment of mixing performance is achieved with the mixing efficiency parameter. In order to experimentally determine the mixing efficiency parameter, the spatial distributions of both mass flux and fuel mass fraction must be measured. In-stream gas sampling techniques are commonly used to measure the fuel mass fraction distribution; however, the mass flux distribution is not easily determined because it requires the measurement of three independent aerothermodynamic variables in addition to the gas composition. Therefore, to experimentally determine the mixing efficiency parameter, the spatial distributions of four independent properties must be measured, with each property generally requiring its own unique probe. Because of this difficulty, it is commonly assumed that alternate metrics, which rely solely on the fuel distribution, are good indicators of mixing performance. However, since these alternate metrics do not provide a mass flux-weighted measure of mixing completeness, they can lead to incorrect conclusions being drawn about the mixing performance of the studied fuel injector configuration. Recognizing this shortcoming, this work proposes two new alternate mixing performance metrics that are easier to obtain than the mixing efficiency parameter. The analytical development of the new metrics, as well as their application to relevant CFD and experimental data of high-speed fuel injector configurations, is presented in this work. For two different experiments, the new metrics are shown to provide an excellent representation of the true mass flux-weighted mixing performance, unlike the traditionally-used alternatives. The results presented herein suggest that the new metrics can serve as accurate surrogates for mixing efficiency in future high-speed fuel/air mixing studies.

I. Introduction

Of the many fluid dynamic challenges that are encountered in scramjet flowpath design, perhaps one of the greatest is the need to achieve rapid fuel/air mixing. The primary difficulty is due to the fact that the flow remains supersonic in the scramjet combustor, thereby drastically limiting the amount of time available for the injected fuel to mix and chemically react. In fact, the rate-limiting step in the fuel injection/mixing/combustion process in a scramjet engine is the mixing of the fuel and air [1]. Therefore, by enhancing the rate at which the fuel and air mix it is possible to both reduce the combustor length and achieve significant gains in engine performance. To this end, past research efforts have devised and studied various fuel/air mixing enhancement strategies and injector configurations for scramjet applications. Many of these strategies have been reviewed previously by Seiner et al. [2], Gutmark et al. [3], and Lee et al. [4]. Despite the advances summarized in these works, further research and development is required in order to design high-speed fuel injection systems that sustain and enhance engine performance across a wide range of flight Mach numbers at both on-design and off-design conditions.

For fuel/air mixing studies, it is necessary to define a metric to compare the mixing performance of different fuel injection concepts. Ideally, this metric should be a one-dimensional parameter (varying only in the primary flow direction) that quantifies the degree of mixing completeness of the fuel/air mixture at any cross-stream plane downstream of the injection location. One metric well suited for fundamental, nonreacting, mixing studies is the mixing efficiency parameter (henceforth referred to simply as "mixing efficiency," for brevity). This mass flux-weighted parameter is

*Research Aerospace Engineer, Hypersonic Airbreathing Propulsion Branch, NASA Langley Research Center, Member AIAA.
†Research Aerospace Engineer, Hypersonic Airbreathing Propulsion Branch, NASA Langley Research Center, Senior Member AIAA.
‡Research Aerospace Engineer, Hypersonic Airbreathing Propulsion Branch, NASA Langley Research Center, Associate Fellow AIAA.

defined as the fraction of the least available reactant that would react if the fuel/air mixture were brought to chemical equilibrium without further mixing [5].

The calculation of mixing efficiency at a given cross-stream plane requires the spatial distributions of both mass flux and fuel mass fraction. In an experiment, although the fuel distribution is relatively straightforward to measure with in-stream gas-sampling techniques, the mass flux distribution is not easily determined; it requires spatially distributed measurements of three independent aerothermodynamic properties, in addition to gas composition. This is most commonly accomplished by augmenting planar gas-sampling data with the spatial distributions of pitot pressure, total temperature, and static pressure measured at the same plane [6]. This method is challenging in practice because each of the four property measurements requires its own uniquely designed measurement probe and many repetitions of the experiment are needed to obtain a sufficiently dense spatial distribution of each property at every downstream plane. This process becomes untenable when several injector configurations must be tested. An alternate method that uses iodine planar laser-induced fluorescence (PLIF) to measure all of the properties required to calculate the mixing efficiency has been demonstrated in the past [7]. However, the implementation of the iodine PLIF technique presents a number of challenges (such as iodine seeding and corrosion issues, a complex optical setup requiring multiple laser sheet directions to measure velocity, and larger uncertainties than intrusive probe-based measurements [8]) that limit its adoption as a standard measurement technique.

Because of the difficulty in experimentally determining the mixing efficiency, a common practice in many fuel/air mixing experiments is to assume that alternate metrics, which rely solely on the fuel distribution, are good indicators of mixing performance. Metrics commonly used for this purpose are the decay of maximum fuel mass fraction, the spatial unmixedness parameter, and various plume area-based metrics [6, 9, 10]. However, because these alternate metrics do not provide a mass flux-weighted measure of mixing performance, they could lead to different conclusions from those based on mixing efficiency. This was demonstrated by the authors in a previous work wherein a variety of alternate mixing performance metrics were calculated from the results of CFD simulations of different injector configurations. This work found that some of the commonly used alternate metrics were better correlated with mixing efficiency than others and, more importantly, which injector was deemed the "better" mixer depended upon which metric was used [11].

Recognizing both the challenge of experimentally determining the mass flux distribution and the potential hazards of the traditional metrics based solely on fuel distribution, the motivation for the present work was to develop a new mixing performance metric. The new metric must meet two criteria: one, it must be easier to obtain than mixing efficiency and, two, it must also be a better representation of the a mass flux-weighted mixing performance than the traditionally used alternatives. Specifically, the new metric must be able to be calculated from the experimental data obtained in the Enhanced Injection and Mixing Project (EIMP), a fuel/air mixing study currently underway at the NASA Langley Research Center. The EIMP [12] is investigating the underlying fundamental physics relevant to fuel injection and mixing for scramjets with flight Mach numbers greater than eight in order to develop mixing enhancement strategies that minimize the total pressure loss incurred during the fuel/air mixing process at the high Mach numbers of interest.

The approach taken by the EIMP utilizes both experiments and computational simulations. The experiments consist of helium injection into a Mach 6 airstream using a test bed platform that accommodates interchangeable fuel injectors. Helium mass fraction, pitot pressure, and total temperature are obtained via in-stream probes in the mixing flowfield downstream of the injectors. The data from the experiments are used to anchor computational fluid dynamics (CFD) simulations which, in turn, are used to provide flowfield details and calculate performance metrics–such as the mixing efficiency. The experimental data were also originally intended to enable rapid screening of fuel injection concepts, however, based on the subsequent findings mentioned above [11], screening and ranking injectors based on the traditionally-used fuel distribution-based mixing metrics would be highly suspect. Therefore, the authors sought to take advantage of the additional flowfield information provided by the measurements of pitot pressure and total temperature to develop a new mixing performance metric that would reliably correlate with mixing efficiency.

It will be shown that two newly proposed metrics not only correlate well with mixing efficiency, but yield remarkably good approximations of the mixing efficiency for the flow conditions and cases investigated thus far for the EIMP. To test the validity of the new metric across a wider range of freestream conditions and injector geometries than those present in the EIMP, it is also applied to a set of data from an earlier, independent, mixing study performed at Mach 2 flow conditions in the Transverse Jet Facility (TJF), also at NASA Langley Research Center [13]. It will be shown that the newly proposed metrics also provide an excellent approximation of mixing efficiency for the TJF data set. Therefore, it is concluded that the metrics' applicability extends beyond the particular conditions of the EIMP, suggesting that they can be used in a wide variety of fundamental fuel/air mixing experiments. The potential impact on such experiments is significant because it enables the accurate determination of mixing performance with a very simplified experimental setup compared to that needed to experimentally determine the true mixing efficiency.

To begin, this work describes the specific test conditions and injector configurations investigated. This is followed by a simple analysis, using only compressible flow relations, to investigate the range of flow conditions under which the new metrics can be expected to yield an acceptable substitute for mixing efficiency. Proof of both metrics' applicability to high-speed fuel/air mixing studies is then demonstrated with the use of both computational (EIMP) and experimental (EIMP and TJF) data.

II. Injector Configurations and Experiment Descriptions

A. Enhanced Injection and Mixing Project

Thus far, three different fuel injectors, a strut, a ramp, and a flushwall injector, have been studied in the EIMP both numerically [14–16] and experimentally [17, 18]. These injectors represent the three basic injector types commonly considered for high speed propulsive flowpaths. The injector configurations tested are derived from configurations previously examined in the literature [19, 20]; however, in the EIMP they are tested at a higher Mach number than those at which they were previously studied in the cited works. This approach is consistent with the primary goal of the EIMP, which is to investigate the fundamental physics of the fuel injection and mixing processes for scramjets with flight Mach numbers greater than eight.

The injectors are experimentally tested in the Arc-Heated Scramjet Test Facility (AHSTF) at the NASA Langley Research Center [21–23]. The heated air has a stagnation pressure of 625 $psia$ and expands through a facility nozzle to an exit Mach number of 6.48 and a Reynolds number of 5×10^6 ft^{-1}. These conditions approximate the combustor entrance conditions of a notional vehicle flying at Mach 15 with a dynamic pressure of 1500 psf. To reduce cost and complexity, the tests are conducted at reduced total temperatures (1310 $^\circ R$ or 1760 $^\circ R$) and with an inert fuel (helium, simulating hydrogen), which allow for uncooled test hardware. The injectors are tested on an open flat plate to allow for easy optical and in-stream probe access to the fuel/air mixing region, but this requires that an intended fueling area (IFA) for each injector configuration be defined in order to set the global equivalence ratio. The impact of the differences between the ground test configuration (reduced total temperature, open flat plate, inert fuel simulant) and the notional flight vehicle configuration (true flight enthalpy, ducted flow path, reacting fuel) on the behavior of the mixing flowfields has been investigated computationally by Drozda et al. [15, 16], which confirmed the practical relevance of the conditions replicated by the simplified experimental setup. Schematics of the three injector configurations are shown in Fig. 1 where the outlined box depicts a single injector's intended fueling area.

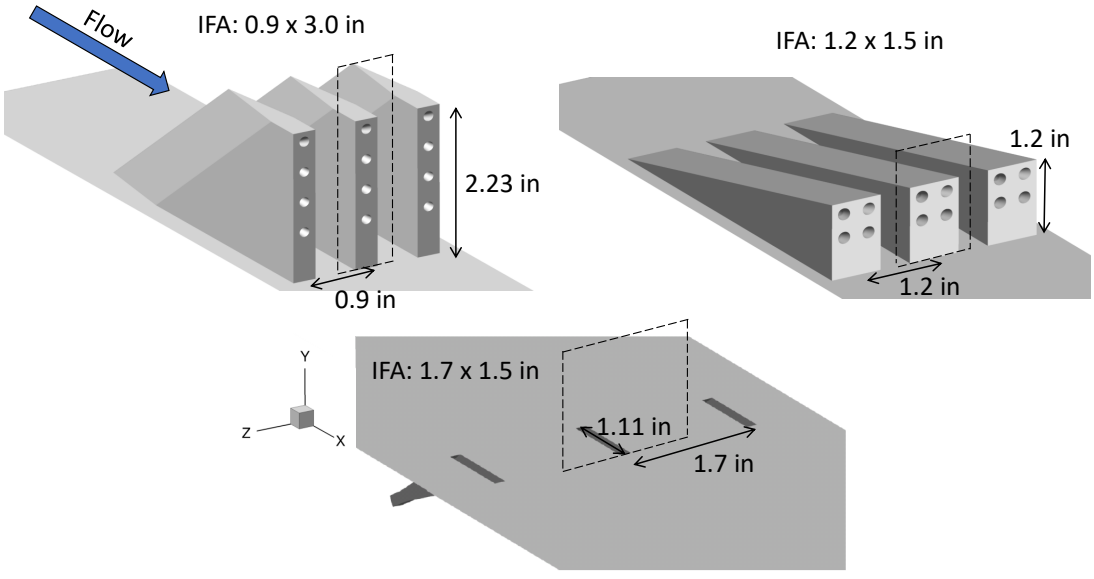

Fig. 1 EIMP injector configurations. Strut (top left), ramp (top right), and flushwall (bottom).

The in-stream measurements of pitot pressure, total temperature, and gas composition are made with probes that can be traversed across any cross-stream plane downstream of the injectors. The pitot pressure and total temperature measurements are made using standard techniques. The gas composition measurements are made with a constant temperature anemometer (CTA)-based gas sampling technique that is commonly used to make concentration measurements in binary gas mixtures [24–27]. For a further description of the experiment, including the test articles and instrumentation hardware, the reader is referred to the work of Cabell et al. [12].

B. Transverse Jet Facility

To test the validity of the newly proposed metrics for injector geometries and freestream flow conditions that are different from those in the EIMP, they are applied to the experimental data set presented in Doerner and Cutler [13]. In Ref. [13], a total of ten different ramp and flushwall injector configurations were used to study the effects of swirling and skewed fuel injection on mixing performance. The experiments were performed in the Transverse Jet Facility at the NASA Langley Research Center. This facility delivers unheated air ($P_0 = 115\ psia$ and $T_0 = 538.2\ ^\circ R$) through a Mach 2 nozzle with an exit cross section of $3.5 \times 1.5\ in^2$ to a rectangular duct test section of the same dimensions. For each configuration studied, an underexpanded helium jet was injected supersonically into the ducted Mach 2 freestream. In these experiments, measurements of the mixing field were made with a pitot probe, a cone static pressure probe, a total temperature probe, and a gas-sampling probe, which used the same CTA-based gas composition measurement technique as the EIMP system. Because four independent properties were measured, all remaining aerothermodynamic variables could be computed. Consequently, the mixing efficiency, η_m, can be calculated from the experimental data and allows for a direct one-to-one comparison with the newly proposed metrics. For further details about these experiments and their conclusions, the reader is referred to Ref. [13].

III. Analysis of the Alternative Mixing Performance Metrics

The mixing efficiency, η_m, is the primary metric used to quantify injector mixing performance in the EIMP because it is a true mass flux-weighted measure of mixing completeness. It is defined as the fraction of least available reactant, α, that would react if the fuel/air mixture were brought to chemical equilibrium without further local or global mixing. The definition used herein is the one proposed by Mao et al. [5], i.e.,

$$\eta_m = \frac{\dot{m}_{\alpha,mixed}}{\dot{m}_{\alpha,total}} = \frac{\int \alpha_R \rho u dA}{\int \alpha \rho u dA}, \tag{1}$$

where,

$$\alpha_R = \begin{cases} \alpha, & \alpha \leq \alpha_{st} \\ \frac{\alpha_{st}}{1-\alpha_{st}}(1-\alpha), & \alpha > \alpha_{st} \end{cases}. \tag{2}$$

In the formulation above, the integration is over a single downstream cross-stream plane and α is either the fuel or oxidizer mass fraction, depending on whether the flow is globally fuel-lean or fuel-rich, respectively. In both the EIMP and TJF experiments, the equivalence ratio is less than or equal to one for each injector configuration. Therefore, in Eqs. 1 and 2, α denotes the mass fraction of helium and α_{st} is taken to be 0.0285, which is the stoichiometric hydrogen mass fraction for hydrogen/air mixtures. The product of ρ, the local density, and u, the component of velocity normal to dA, is the mass flow per unit area, i.e., the mass flux. The mixing efficiency varies from 0 to 1 with $\eta_m = 0$ corresponding to a completely segregated mixture and $\eta_m = 1$ corresponding to a perfectly mixed mixture.

As mentioned previously, practical challenges of obtaining in-stream distributions of three independent aerothermodynamic variables, in addition to gas composition, often prevent the experimental determination of the mass flux, ρu, and, therefore, the mixing efficiency. This is the case for the EIMP, where the measurements consist only of pitot pressure, total temperature and gas composition. Since one intent of the EIMP experiments is to enable rapid screening of injectors based on the obtained fuel distributions, the authors previously sought to find a metric based solely upon fuel distribution that correlates strongly with mixing efficiency, but none proved satisfactory [11]. Thus, it was clear a new metric had to be developed in order to experimentally characterize the EIMP injectors' mixing performance. This process began by asking: of the parameters that *are* measured or can be calculated from the EIMP experiments, is there one that is proportional to ρu that could be substituted in its stead in Eq. 1 to yield a new mixing metric that approximates η_m better than the previously investigated alternatives?

To answer this question, it is instructive to express ρu in terms of the parameters that are measured in the experiment. Using the ideal gas law and the definition for the speed of sound in a thermally perfect gas, mass flux is first written as:

$$\rho u = \frac{P}{\sqrt{RT}} M \sqrt{\gamma}. \tag{3}$$

Note that because the flowfield is a binary mixture of helium and air, the specific gas constant, R, is known from the helium mass fraction measurement. For illustrative purposes, we invoke the calorically perfect gas assumption to relate the static properties to stagnation properties, denoted with the subscript "0". The subscript "2" has been used to indicate properties downstream of a normal shock. Quantities without the subscript "2" are the same on both sides of the normal shock in a calorically perfect flow. After making use of the calorically perfect gas relations, Eq. 3 becomes:

$$\rho u = \frac{P_{0,2}}{\sqrt{RT_0}} \left[\sqrt{\gamma} M_2 \left(1 + \frac{\gamma - 1}{2} M_2^2 \right)^{\frac{-(\gamma+1)}{2(\gamma-1)}} \right], \tag{4}$$

where all the parameters outside the square brackets are known from the EIMP experiments. Thus, it can be seen that the mass flux is directly proportional to any factor of the quantity $\frac{P_{0,2}}{\sqrt{RT_0}}$. Despite the fact that the calorically perfect gas assumption was used to derive Eq. 4, the proportionality still holds for a calorically imperfect gas because the stagnation properties are still directly proportional to the static properties, even if they cannot be related in closed form. Because of this proportionality, the authors proposed to investigate any parameter that is a factor of $\frac{P_{0,2}}{\sqrt{RT_0}}$ as a substitute for ρu in Eq. 1. Examination of Eq. 1 reveals that if the ratio of mass flux to that parameter is nearly constant across each downstream plane at which η_m is calculated, this would yield a valid approximation of η_m. The parameter proposed for initial investigation was pitot pressure. This was based upon the authors' past experience in comparing scramjet engine data from various ground test facilities with a range of freestream conditions and test gases where it was observed that the ratio of inlet captured mass flux from one facility or condition to another was nearly identical to the ratio of inlet pitot pressure. This suggested that mass flux is a strong function of pitot pressure and that by substituting pitot pressure for mass flux in Eq. 1, a reliable approximation for mixing efficiency could potentially be developed. If this is done, then the proposed alternative metric is:

$$\eta_m^{P_{0,2}} = \frac{\int \alpha_R P_{0,2} dA}{\int \alpha P_{0,2} dA}, \tag{5}$$

and we require:

$$\frac{\rho u}{P_{0,2}} = \frac{1}{\sqrt{RT_0}} \left[\sqrt{\gamma} M_2 \left(1 + \frac{\gamma - 1}{2} M_2^2 \right)^{\frac{-(\gamma+1)}{2(\gamma-1)}} \right] \approx C. \tag{6}$$

However, this is not a realistic general expectation for a complex supersonic mixing flowfield. It is important to note that this requirement needs only to hold true in the actual fuel/air mixing region, as regions of pure fuel or pure air correspond to $\alpha_R = 0$ and, therefore, contribute nothing to η_m. The range of conditions for which $\frac{\rho u}{P_{0,2}}$ is approximately constant can be investigated by plotting $\frac{\rho u}{P_{0,2}}$ as a function of upstream Mach number, M_1, noting that $M_2 = f(M_1, \gamma)$, for a given gas (γ and R) and total temperature. Such a plot is shown in Fig. 2a for a range of gases that have typically been used in fundamental mixing experiments. Many of these studies, like the EIMP, have used helium to simulate hydrogen fuel [6, 13, 28, 29], while some have simply injected hydrogen at conditions that did not promote chemical reaction [30]. Other experiments have studied the mixing of hydrocarbons such as methane [10] or ethylene [10, 31] in nonreacting environments, while others have used heavier fuel surrogates, such as argon [32] or carbon dioxide [33], to simulate hydrocarbon fuels. For simplicity, this plot was generated using calorically perfect relations with all gases at the same total temperature of 540 $^\circ R$, since many of the cited studies were performed "cold" with both the fuel and air near room temperature. However, the effect of a higher total temperature for any gas can easily be understood as a lowering of the values in the curves by a factor of $\sqrt{540/T_0}$, where the total temperature is expressed in degrees Rankine.

Figure 2a shows that as the Mach number increases, $\frac{\rho u}{P_{0,2}}$ asymptotically approaches constant, but unique, values for each gas at a given total temperature. Above Mach 3, the ratio is nearly constant and can be assumed to be, approximately, independent of Mach number. In the fuel/air mixing region, the range of possible values of $\frac{\rho u}{P_{0,2}}$ should be bounded by the curves for pure air and pure fuel at their respective total temperatures. What cannot be depicted in Fig. 2a is that, as the flow mixes, both the fuel mass fraction and flow total temperature should become more uniform, which will

further narrow the possible range of $\frac{\rho u}{P_{0,2}}$ in the mixing region. As seen in Fig. 2a, when cold flow mixing experiments utilize nonreacting hydrocarbons, or hydrocarbon surrogates, the difference in $\frac{\rho u}{P_{0,2}}$ between the pure fuel and air is small compared to that for helium or nonreacting hydrogen. This suggests that the use of the $\eta_m^{P_{0,2}}$ metric is valid in these experiments as long as the Mach number is greater than ≈ 3, or does not vary greatly across a given downstream plane as this Mach number range restriction need only be within a given cross-stream plane where $\eta_m^{P_{0,2}}$ is calculated. However, this does not mean that experiments studying the mixing of light gases with air cannot use the $\eta_m^{P_{0,2}}$ metric when both gases have the same total temperature. First, the mixing performance of an injector will most likely be assessed at some downstream distance where the fuel and air have had a chance to mix, and as explained previously, the variation in $\frac{\rho u}{P_{0,2}}$ across the mixing region will have decreased. Secondly, because $\frac{\rho u}{P_{0,2}}$ of a mixture is a mass-weighted term, its value will rapidly skew toward the value for pure air with fairly little mixing on a molar basis due to the large difference in molecular weights between helium and air.

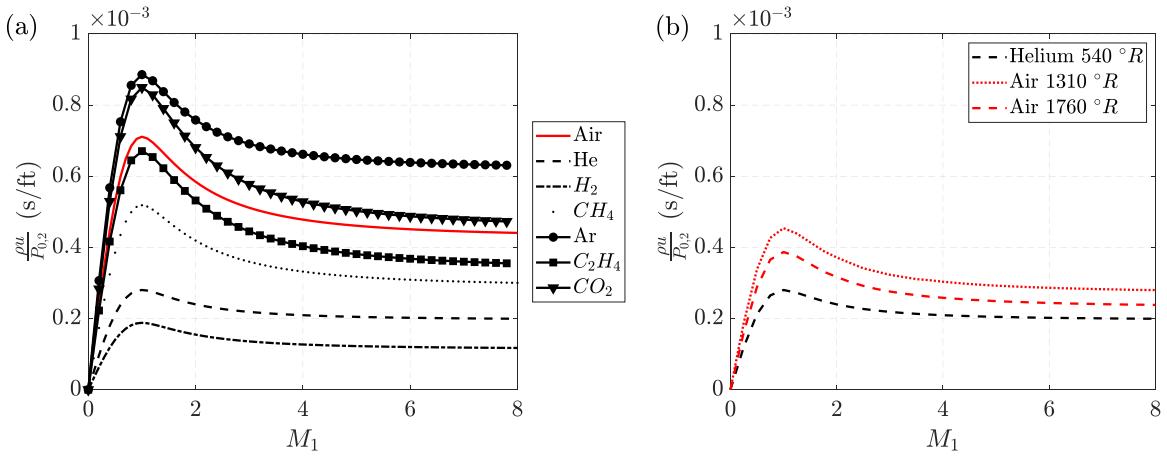

Fig. 2 (a) $\frac{\rho u}{P_{0,2}}$ vs. Mach number for various gases at $T_0 = 540\ ^\circ R$, and (b) $\frac{\rho u}{P_{0,2}}$ vs. Mach number for conditions relevant to the EIMP.

Figure 2b shows the variation of $\frac{\rho u}{P_{0,2}}$ as a function of Mach number for the two gases and total temperatures relevant to the EIMP: pure helium, which is injected with $T_0 = 540\ ^\circ R$, and pure air at both $T_0 = 1310\ ^\circ R$ and $T_0 = 1760\ ^\circ R$, as the experiments can be conducted with the freestream air at either total temperature. Here, $\frac{\rho u}{P_{0,2}}$ was calculated without the calorically perfect gas assumption. The effect of increased air total temperature can be seen by comparing the two curves at $T_0 = 1310\ ^\circ R$ and $T_0 = 1760\ ^\circ R$ with each other and to the curve at $T_0 = 540\ ^\circ R$ in Fig. 2a. The possible range of values in the mixing region, bounded by the curves for fuel and air, has been greatly reduced with the increased air total temperature. Given the Mach 6 inflow of the EIMP, it is expected that a vast majority of the flowfield will have Mach numbers greater than 3. Therefore, using the asymptotes that are approached by each curve, the maximum expected variation in $\frac{\rho u}{P_{0,2}}$ is 17% when the air total temperature is $1310\ ^\circ R$ and is 9% when the air total temperature is $1760\ ^\circ R$. Again, as the flow mixes, both the fuel mass fraction and flow total temperature should become more uniform, which will further narrow the possible range of $\frac{\rho u}{P_{0,2}}$. The effect of the increased total temperature of the air, which serves to decrease the maximum expected variation in $\frac{\rho u}{P_{0,2}}$ across the mixing region, highlights the fact that in the future it could be possible to tailor the total temperatures of the injected fuel and air in order to minimize the variation in $\frac{\rho u}{P_{0,2}}$, which would minimize the potential differences between $\eta_m^{P_{0,2}}$ and η_m.

In summary, two conditions have been identified that must be met in order for the assumption of $\frac{\rho u}{P_{0,2}} \approx C$ to be valid. One, there must be sufficient mixing such that the possible range of $\frac{\rho u}{P_{0,2}}$ lies within a narrow band between the bounding fuel and air curves; and, two, the Mach number in a given cross-stream plane at which $\eta_m^{P_{0,2}}$ is calculated must be greater than 3 or, if the Mach number is less than 3, its range must be sufficiently small such that the variation in $\frac{\rho u}{P_{0,2}}$ due specifically to the influence of Mach number is also small. Although the findings from this simple analysis have shed light on the conditions under which it might be possible to approximate $\frac{\rho u}{P_{0,2}}$ as constant, it remains to be

determined how much it varies during the mixing process in an actual, highly complex, supersonic flow. This is easily accomplished using the results of CFD simulations for the specific conditions in the EIMP and can also be done by performing pretest CFD for any experiment in which the applicability of this metric is of interest.

As noted above, the quantity $\frac{P_{0,2}}{\sqrt{RT_0}}$ and any of its factors (i.e., $\frac{P_{0,2}}{\sqrt{T_0}}$, $\frac{1}{\sqrt{RT_0}}$, etc.) are also directly proportional to mass flux and could be considered as a replacement for ρu in Eq. 1. Although a similar analysis with results analogous to those of Fig. 2 could be carried out for any of the aforementioned factors, the approach taken by the authors was to investigate each factor of $\frac{P_{0,2}}{\sqrt{RT_0}}$ directly by calculating its associated substitute mixing performance metric from the available EIMP CFD results. As will be shown in later sections, there are two metrics that yield remarkably good approximations of the mixing efficiency. These are the previously discussed $\eta_m^{P_{0,2}}$ and the metric obtained by substituting $R^{-1/2}$ for mass flux in Eq. 1, or η_m^R. The latter is of particular interest since flowfields of typical nonreacting mixing experiments are treated as binary mixtures of fuel and air and the local value of the specific gas constant, R, can be calculated simply from the measurement of the fuel mass fraction. Therefore, η_m^R is solely dependent upon the measured fuel distribution and, thus, requires fewer measurements than either η_m or $\eta_m^{P_{0,2}}$. The extent to which both $\eta_m^{P_{0,2}}$ and η_m^R can serve as reliable approximations for mixing efficiency in the EIMP is demonstrated with both CFD and experimental data subsequently in Sec. IV and Sec. VA. Section VB uses the data from the TJF mixing experiments to investigate the applicability of both metrics under conditions of lower inflow Mach number where the injected helium fuel and freestream air have the same total temperature.

IV. Application to EIMP CFD Data

The numerical simulations were completed pretest with boundary conditions consistent with the 1760 $^\circ R$ total temperature experimental ground test condition. They were performed using the Viscous Upwind aLgorithm for Complex flow ANalysis (VULCAN-CFD) code [34]. VULCAN-CFD is a multiblock, structured-grid, cell-centered, finite-volume solver widely used for all-speed flow simulations. For this work, Reynolds-averaged simulations were performed. For further information on the CFD simulations, including the specific details of the numerical schemes used, the reader is referred to the previous works of Drozda et al. [14–16]. In order to familiarize the reader with the general flow features of the EIMP's strut, ramp, and flushwall injectors, contour plots of Mach number are shown in Fig. 3. In this figure, the solid black lines denote the stoichiometric value of the fuel mass fraction and show how the shape of the injected fuel plume evolves downstream.

From Fig. 3, it can be gleaned that the three different injector types each act in a different manner to mix the injected fuel with the surrounding air. The strut injector serves primarily as a fuel placement device, protruding into the flow to place fuel directly into the core of the incoming airstream. The ramp injector's main purpose is to augment the fuel mixing process by introducing large-scale streamwise vortices that enlarge and stretch the fuel/air interface, which it does by shedding a counterrotating vortex pair (CVP) from its upper surface. Like the ramp injector, the flushwall injector serves to introduce vorticity into the mixing field; however, instead of accomplishing this task with a physical body placed in the flow, the vortical motion is created by the interaction of the injected fuel jet with the freestream. Due to the differences in wetted surface area and projected frontal area, each injector will also produce different amounts of total pressure loss (i.e., drag) in addition to different mixing performance. Though injector drag must undoubtedly be taken into account during the design of any realistic injector system, the focus of this work is solely on the quantification of mixing performance. For a more detailed discussion on the different physical flow features and performance of the different injectors, the reader is referred to Drozda et al. [14].

Shown in Fig. 4 are a collection of mixing performance metrics calculated from the CFD simulations of the strut, ramp, and flushwall injector configurations plotted versus x, the distance downstream from the injection plane. Figure 4a depicts the mixing efficiency, η_m and the remaining subfigures, Figs. 4b–f depict traditionally used alternate mixing performance metrics that are calculated solely from the spatial distribution of the fuel mass fraction. These metrics are one minus the maximum helium mole fraction, $1 - \chi_{he,\,max}$; one minus the spatial unmixedness parameter, $1 - U_s$; relative fuel plume area, $\bar{A}$; fuel plume area normalized by the intended fueling area, A_p/IFA; and the flammable plume fraction, A_f/A_p, respectively. The complete definitions of each of these metrics can be found in the authors' previous work [11]. Fig. 4 shows that conclusions differing from those based on mixing efficiency, about both the rate of mixing and the overall ranking of the best mixing configuration, can be made depending upon which alternative performance metric is used. For example, the initial rate of mixing indicated by the maximum helium mole fraction and the spatial unmixedness parameter, Figs. 4b and c, is much higher than that indicated by the fuel plume area-based metrics, Figs. 4d–f, which are closer to the initial mixing rates displayed by mixing efficiency. If the three injectors

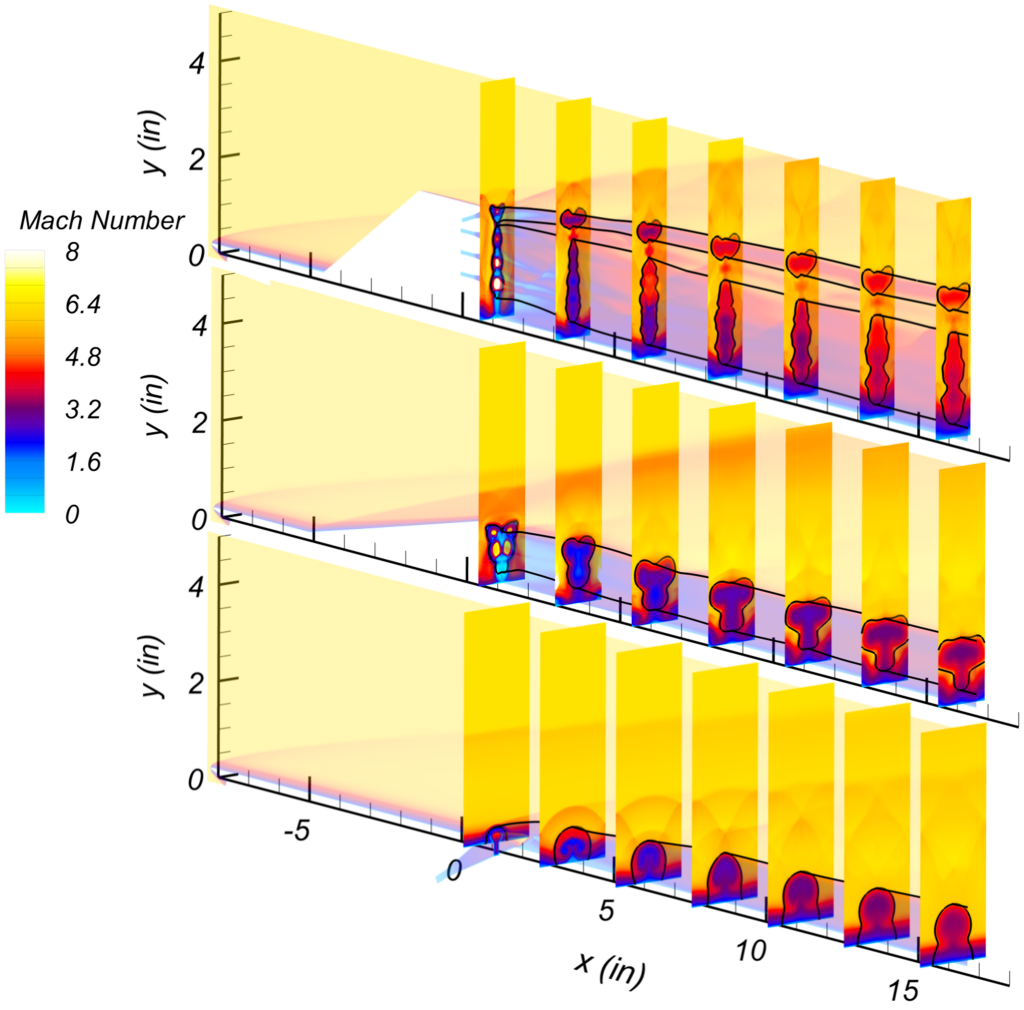

Fig. 3 Mach number contours for the strut (top), ramp (middle), and flushwall (bottom) injector configurations. The black lines denote the stoichiometric value of the fuel mass fraction.

were ranked based upon any of the alternate mixing performance metrics, only flammable plume fraction, Fig. 4f, would correctly rank the injectors. However, the relative performance differences between the injectors (i.e., how much better one injector is than another) would not be correctly conveyed. These contradictions highlight the most important conclusions from Ground et al. [11].

Figure. 5 shows that these issues are remedied by both the $\eta_m^{P_{0,2}}$ and η_m^R metrics. In Figs. 5a and c the solid lines represent η_m, and the symbols represent $\eta_m^{P_{0,2}}$ or η_m^R, respectively. Figures 5b and d depict the absolute value of the differences between the two new metrics and the mixing efficiency. Overall, there is a remarkably high level of agreement between η_m and $\eta_m^{P_{0,2}}$ across the entire flowfield for each injector configuration, with the maximum difference between them never exceeding 0.01. The maximum difference between η_m and $\eta_m^{P_{0,2}}$ is seen within the first five inches of the injection location, after which the difference between η_m and $\eta_m^{P_{0,2}}$ is less than 3% for the flushwall injector and less than 1.5% for the strut and ramp injectors. It will be shown later that these differences are smaller than the measurement uncertainty of the $\eta_m^{P_{0,2}}$ metric measured in the EIMP experiments, which makes $\eta_m^{P_{0,2}}$ virtually indistinguishable from η_m for the flow conditions and injector geometries of the EIMP. Figure 5d shows that, while η_m^R is not as accurate a representation of mixing efficiency as $\eta_m^{P_{0,2}}$ is, it is still accurate enough to distinguish the relative differences in mixing performance between the three different injector configurations. This stands in stark contrast to the traditionally used fuel distribution based mixing performance metrics depicted in Figure 4, which are not able to accomplish this task.

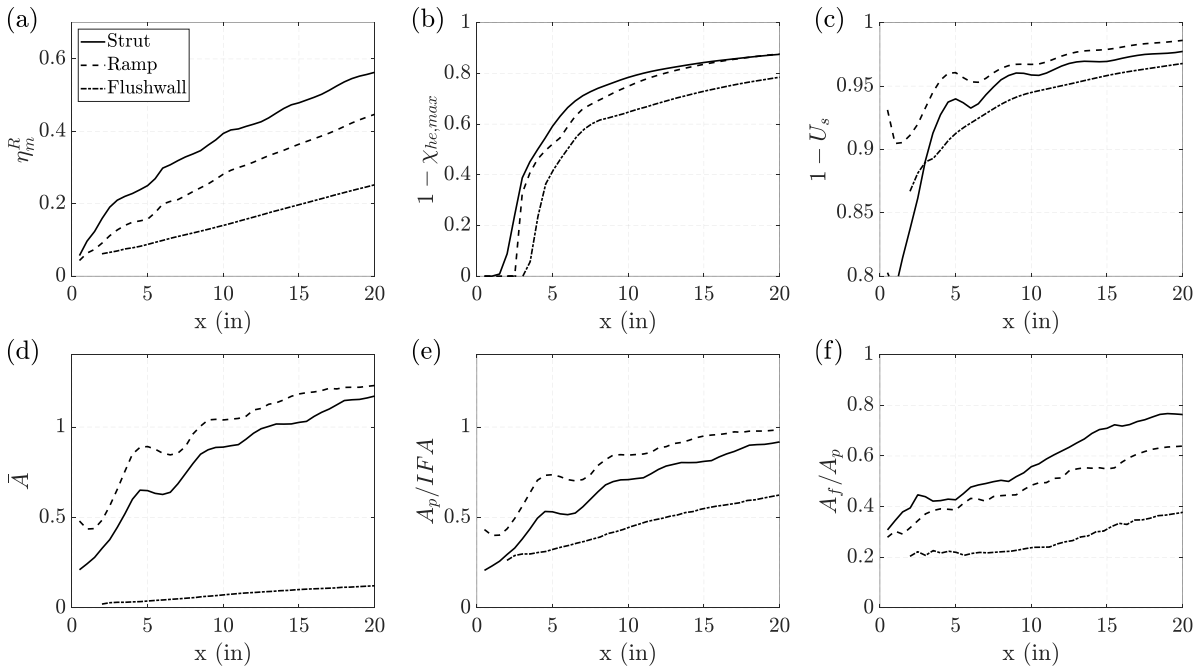

Fig. 4 CFD predicted mixing performance metrics. (a) η_m, (b) one minus the maximum helium mole fraction, (c) one minus the spatial unmixedness parameter, (d) relative fuel plume area, (e) plume area normalized by the intended fueling area, and (f) flammable plume fraction.

V. Application to Experimental Data

A. Enhanced Injection and Mixing Project

To date, experimental data has been collected at the low temperature test condition ($T_0 = 1310°R$) for the strut injector at five planes that are $x = 0.5, 1, 2, 4$ and 6 $in.$ downstream of the injection location. For each of the planes surveyed, measurements were acquired in a grid with a nominal $1/8$ $in.$ by $1/8$ $in.$ spacing in the y and z directions, respectively. The resulting contours of helium mole fraction and pitot pressure are shown in Fig. 6. Post-test CFD simulations at the low temperature test condition are not yet available for direct comparison. An in-depth comparison between the CFD and experimental results will be the focus of a future work. Nonetheless, the experimental results show that, qualitatively, the fuel plume evolves as expected from the pretest CFD predictions at the high temperature test condition ($T_0 = 1760°R$) shown in Fig. 3.

The data of Fig. 6 were used to calculate the experimentally derived values of $\eta_m^{P_{0,2}}$ and η_m^R at each survey location. Results are shown in Fig. 7 along with the results from the pretest CFD for reference. The experimental results include uncertainty bars indicating the 95% confidence interval on the experimentally measured metrics. The uncertainty analysis used Monte Carlo methods to propagate the systematic and random uncertainties of every measurement, including uncertainties from the hot-wire calibration procedure, into an uncertainty in the fuel mole fraction and pitot pressure at each individual location in the measurement plane. The uncertainties in fuel mole fraction and pitot pressure at every location in the measurement plane contribute to the overall uncertainty in the experimental metrics, which is slightly different for each measured plane. In each plane, the uncertainty in $\eta_m^{P_{0,2}}$ is larger than the difference between η_m and $\eta_m^{P_{0,2}}$ in the CFD data, shown in Fig. 5b. Therefore, even if enough variables were measured to calculate mixing efficiency from the experimental data, η_m and $\eta_m^{P_{0,2}}$ would be indistinguishable from one another given their respective uncertainties for the EIMP conditions. In fact, it is highly probable that η_m would have a larger uncertainty than $\eta_m^{P_{0,2}}$ due to the fact that the measurement uncertainty from two additional variables (the spatial distributions of total temperature and static pressure) would propagate into the result. This could be another potential benefit of the $\eta_m^{P_{0,2}}$ metric. Like $\eta_m^{P_{0,2}}$, η_m^R can be measured with a small enough uncertainty to be able to rank injector performance experimentally. However, due to the larger difference between the values of η_m and η_m^R shown in Fig. 5d, it is conceivable

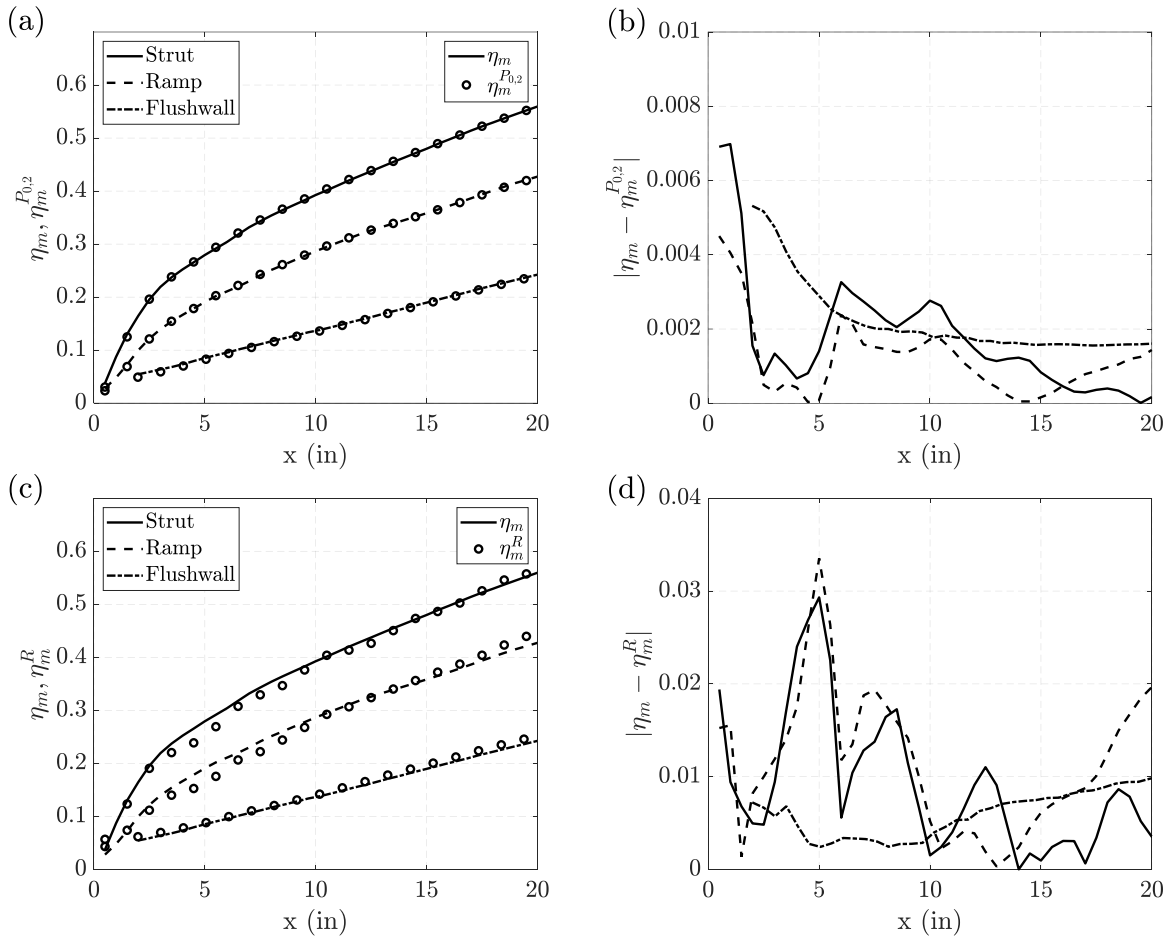

Fig. 5 Comparison of η_m and the newly proposed mixing metrics in the EIMP CFD data. (a) Raw metric values. η_m is represented by the lines and $\eta_m^{P_{0,2}}$ by the symbols. (b) Absolute value of the difference between η_m and $\eta_m^{P_{0,2}}$ (c) Raw metric values. η_m is represented by the lines and η_m^R by the symbols. (d) Absolute value of the difference between η_m and η_m^R.

that a more accurate determination of mixing performance could be made by experimentally determining the mixing efficiency–though this would come at the cost of needing to measure the spatial distributions of three additional variables at each interrogated plane.

Two points must be made prior to comparing the experimentally calculated $\eta_m^{P_{0,2}}$ and η_m^R profiles with those from the CFD simulations. First, although the pretest CFD is for a higher temperature condition, it nevertheless provides a valuable comparison because the difference in total temperature between the two conditions is expected to have only a slight effect on the mixing efficiency[35]. Second, it is important to use the coarsened experimental grid resolution, where the data are sampled exactly at the experimental measurement locations, as differences in the metrics from the full and reduced resolution CFD can be significant. The important conclusion to draw from the results shown in Fig. 7 is that it is possible to measure both of the newly proposed metrics with low enough measurement uncertainty to capture the trend identified in the CFD data.

These results, taken together with the results presented in Sec. IV, clearly demonstrate the superiority of the two newly proposed mixing performance metrics over the historically-used alternatives to mixing efficiency. To calculate $\eta_m^{P_{0,2}}$, the spatial distribution of only one other variable, pitot pressure, is required to be measured in addition to the fuel mass fraction distribution. Thus, this metric achieves the primary goal stated at the outset of this effort, which was to define a metric that is easier to obtain than mixing efficiency while also being a more accurate representation of the

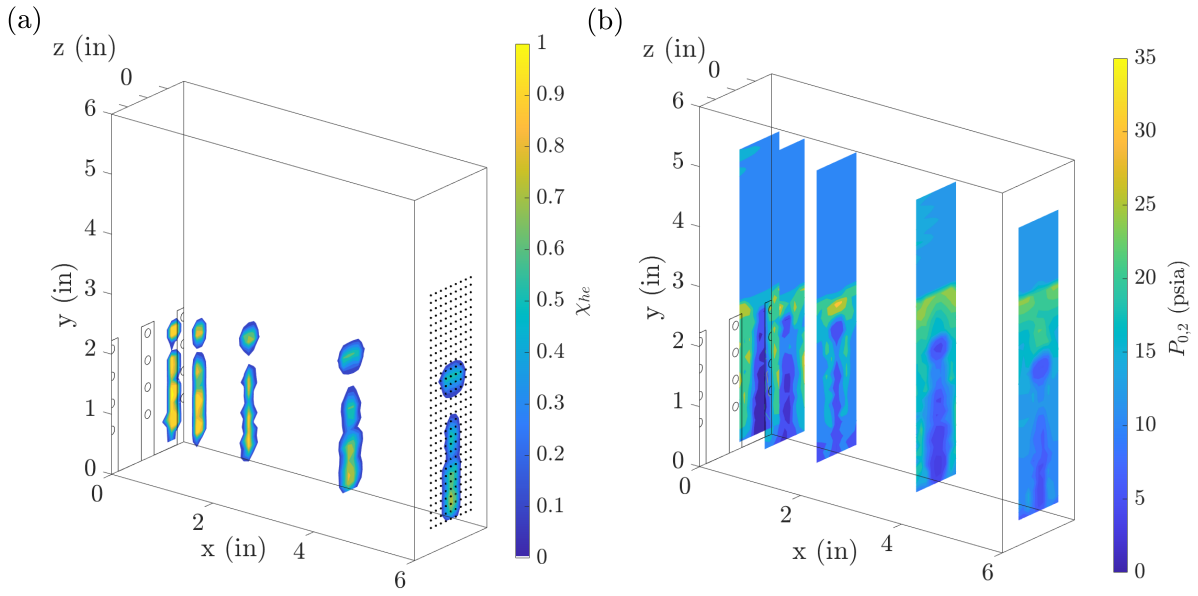

Fig. 6 Experimental data contours at $x = 0.5, 1, 2, 4$ and 6 *in.* of (a) Helium mole fraction, and (b) pitot pressure. At the $x = 6$ *in.* station, the nominal experimental sampling grid is depicted.

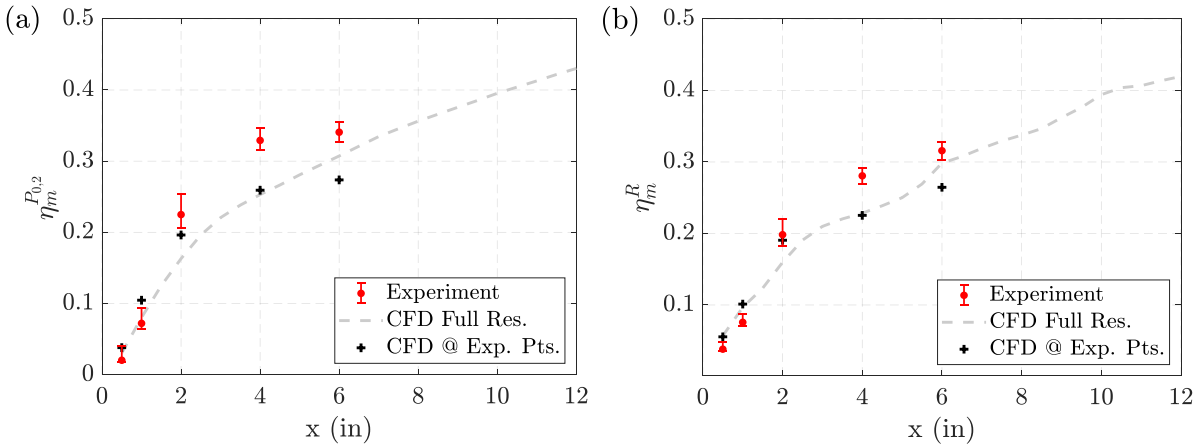

Fig. 7 (a) Plot of $\eta_m^{P_{0,2}}$ from experimental data, and (b) Plot of η_m^R from experimental data. CFD comparisons are shown for reference.

mass flux-weighted mixing performance than the traditional fuel distribution-based surrogates. Despite being solely based upon the fuel distribution, η_m^R provides a good approximation of mixing efficiency–one that is significantly better than any of the other fuel distribution-based metrics used in the past. Therefore, even though Fig. 5d shows it to have a slightly larger deviation from mixing efficiency than $\eta_m^{P_{0,2}}$, the fact that it requires only the experimental measurement of the fuel mass fraction distribution could make it preferable to $\eta_m^{P_{0,2}}$ in some situations. The following section investigates whether these newly introduced metrics also yield a good approximation for η_m when applied to the TJF data set.

B. Transverse Jet Facility

As mentioned in Sec. IIB, Doerner and Cutler [13] studied a total of ten different ramp and flushwall injector configurations in order to investigate the effects of swirling and skewed fuel injection on mixing performance. Here, two of these configurations are used to discuss the applicability of the $\eta_m^{P_{0,2}}$ and η_m^R metrics to the TJF data. They are: (1) the no swirl, 0° skew flushwall injector (designated *N0*) and (2) the swirling injection, 25° skew flushwall injector (designated *S25*). The two injectors were probed at stations 1, 5, and 9 *in*. downstream of the injection location, respectively. Although no CFD simulations of the TJF experiments are available to calculate and compare metrics, recall that enough independent measurements were made to calculate both η_m and the proposed alternatives from the experimental data. Fig. 8 depicts the comparison of the metrics to mixing efficiency in the selected TJF data. Ref. [13] estimates the uncertainty in η_m to be ±5%.

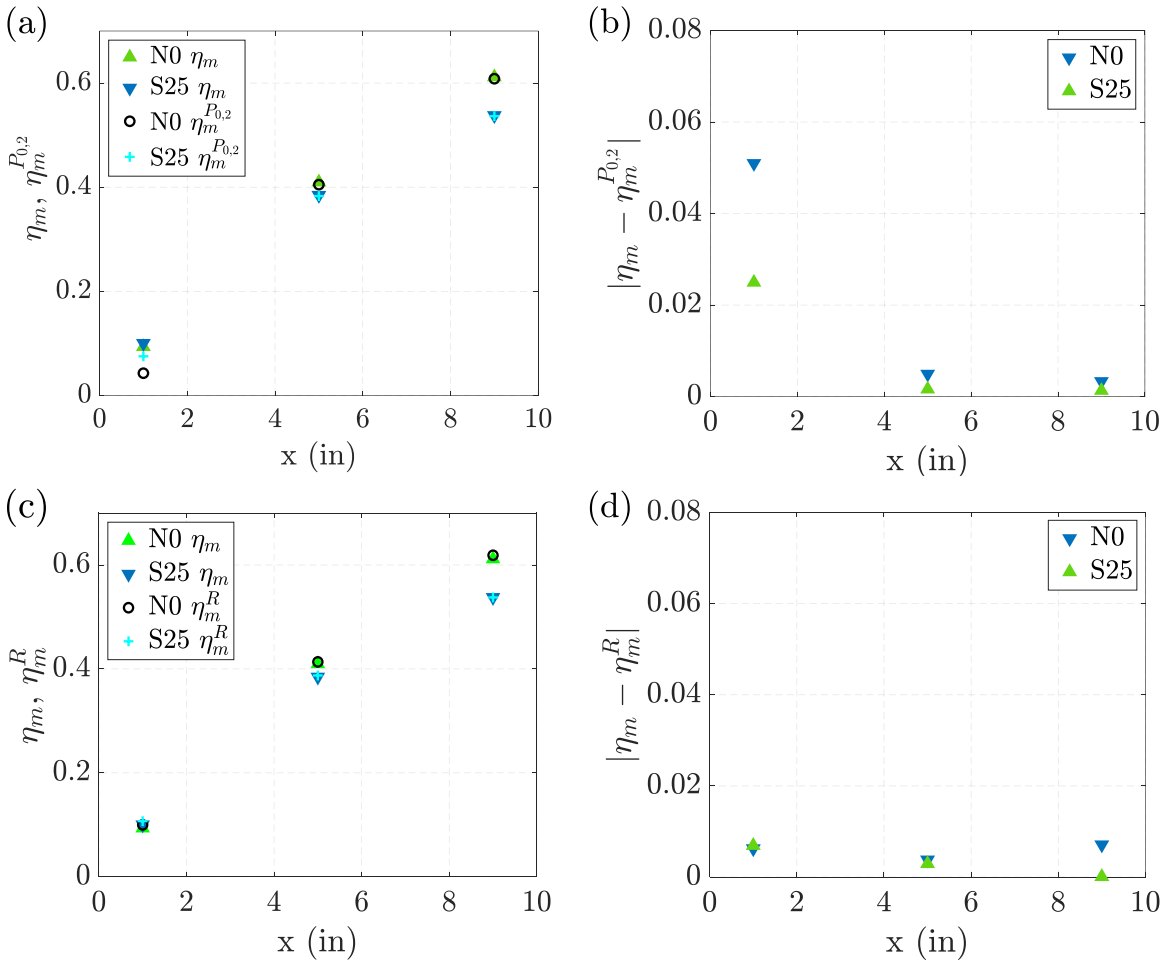

Fig. 8 Comparison of metrics in the TJF data. (a) η_m and $\eta_m^{P_{0,2}}$, (b) absolute value of the difference between η_m and $\eta_m^{P_{0,2}}$, (c) η_m and η_m^R, and (d) absolute value of the difference between η_m and η_m^R.

At the 5 and 9 *in*. downstream stations, the agreement between η_m and $\eta_m^{P_{0,2}}$ is on par with that seen between the two metrics in the EIMP CFD data in Fig. 5b, with differences less than 0.005 between them. However, at the 1 *in*. station, the differences are more pronounced–with a difference of 0.051 between the two metrics for the *N0* injector and 0.025 for the *S25* injector. The magnitude of these differences results in an underprediction of the mixing performance by the $\eta_m^{P_{0,2}}$ metric by approximately 54% and 25% for the *N0* and *S25* injectors, respectively, at the nearfield station. To illustrate the reason for this discrepancy, the contours of helium mole fraction and Mach number are shown for the *N0* injector in Fig. 9. At the farthest two downstream stations, where there is negligible difference between η_m and $\eta_m^{P_{0,2}}$,

the Mach number in the fuel plume is quite uniform–between Mach 1.6 and Mach 1.8 even though the helium and air have yet to completely mix. From the data presented in Fig. 8, it can be concluded that the amount of mixing present at these two stations is sufficient for pitot pressure to reliably approximate mass flux, thereby allowing for $\eta_m^{P_{0,2}}$ to serve as a dependable quantitative metric of mixing completeness. On the other hand, at the 1 $in.$ station, there is both a large range in the Mach number within the fuel plume, between Mach 1.4 and Mach 3.6, and high helium mole fraction values, a maximum of 0.98, because the fuel has had very little time to mix with the surrounding air. Referring back to Fig. 2b, both the wide range of low supersonic Mach numbers and the presence of a large area of relatively unmixed helium within the fuel plume will result in a larger spread in the values of $\frac{\rho u}{P_{0,2}}$, making the assumption that this ratio is approximately constant much less accurate at the 1 $in.$ station. Although not shown here, a similar scenario exists at the 1 $in.$ station of the *S25* injector. However, the range of Mach numbers in the fuel plume is smaller (between Mach 1.5 and 2.5), which results in a smaller difference between η_m and $\eta_m^{P_{0,2}}$ compared to the *N0* injector.

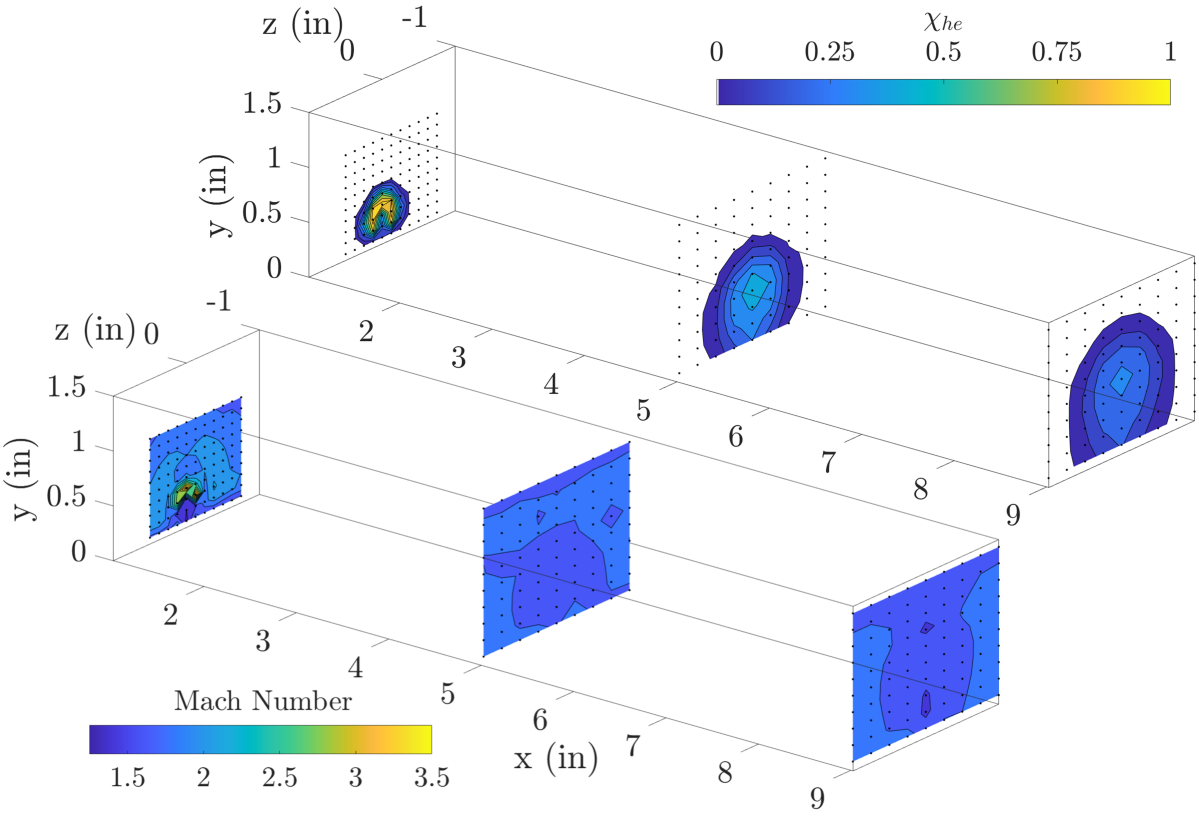

Fig. 9 Contours of helium mole fraction (top) and Mach number (bottom) for the *N0* injector of the TJF mixing experiments. The experimental sampling grid is depicted at each station.

Figures 8c and d show that the η_m^R metric is also a very good approximation for mixing efficiency in the TJF data. In fact, the difference between η_m and η_m^R in these measurements is slightly less than the difference seen between the same two metrics in the EIMP CFD data presented in Fig. 5d. More importantly, the η_m^R metric is a much more accurate representation of mixing efficiency than $\eta_m^{P_{0,2}}$ at the x = 1 $in.$ station for the TJF injectors. The reason for this is still under investigation.

It is important to note that of the ten total injector configurations studied in Ref. [13], only the two discussed herein probed the 1 $in.$ station. The remaining injectors were probed at only the 5 and 9 $in.$ stations. Though the data from the other eight injectors are not presented herein, the differences between η_m and the newly proposed metrics were assessed for each configuration. Similar to the comparison of the metrics shown for the *N0* and *S25* injectors, the difference between the new metrics and η_m at both the 5 and 9 $in.$ stations is very small–less than 0.015 for both metrics for all eight of the other injectors studied in the TJF. Unfortunately, in none of the configurations studied were any stations

between 1 and 5 $in.$ probed, so it is not possible to state at what distance downstream from the injection location $\eta_m^{P_{0,2}}$ becomes an acceptable approximation of η_m. However, as was mentioned previously, the mixing performance of an injector will most likely be assessed at distances far enough downstream for this approximation to be valid. To this end, all ten of the injectors studied in Ref. [13] were ranked at the 9 $in.$ station according to the mixing efficiency, η_m, the newly proposed $\eta_m^{P_{0,2}}$ and η_m^R metrics, and the five traditionally-used fuel distribution-based metrics presented in Fig. 4. Of these seven alternatives, only $\eta_m^{P_{0,2}}$ and η_m^R rank the injectors in the same order that they would be ranked by mixing efficiency. This is notable for the $\eta_m^{P_{0,2}}$ metric because the TJF has, according to Fig. 2b, flow conditions that present one of the more challenging environments for $\frac{\rho u}{P_{0,2}}$ to be assumed constant. Likewise, this fact is notable for the η_m^R metric because a metric based solely on the measured fuel distribution was able to correctly rank the injectors according to their mixing performance, something no other fuel distribution-based metric was able to achieve. The fact that these two metrics perform as demonstrated in the two largely different freestream environments of the EIMP and TJF, speaks favorably towards their applicability across a wide range of fundamental fuel/air mixing studies of high-speed injector configurations.

VI. Conclusions

This work has tackled a common challenge in high-speed fuel/air mixing experiments. In these experiments the parameter that most reliably quantifies fuel/air mixing performance, the mixing efficiency parameter, is difficult to obtain because it requires the measurement of the spatial distributions of mass flux and fuel mass fraction. The primary difficulty lies in obtaining the spatial distribution of mass flux, which requires the measurement of three independent aerothermodynamic quantities in addition to fuel mass fraction. Typically, to lessen the burden of an experimental injector characterization, alternate metrics based solely upon the measured fuel distribution are used to experimentally quantify injector performance. The problem with the traditionally-used alternatives is that they can lead to incorrect conclusions about an injector's mixing ability, as proven by the authors' previous work.

To remedy this issue, this work has proposed two new alternate mixing performance metrics, denoted $\eta_m^{P_{0,2}}$ and η_m^R. These metrics substitute either pitot pressure or $R^{-1/2}$ for mass flux in the mixing efficiency equation and, thus, require the spatial distributions of fewer parameters (one or two) to be measured for their calculation than mixing efficiency (four). The analytical reasoning behind these metrics was presented, as well as their application to two separate high-speed fuel/air mixing studies that have taken place at the NASA Langley Research Center. The application of the metrics to the current Enhanced Injection and Mixing Project (in both computational and experimental data) and previous experiments performed in the Transverse Jet Facility, have proven their validity as quantitative measures of mass flux-weighted mixing performance for different types of injectors and two different Mach number ranges.

The development of these new mixing performance metrics is beneficial in several ways. First off, specific to the EIMP, they enable the screening and ranking of injectors solely from the EIMP experimental data, which was an original goal of the project. Additionally, the metrics have the added benefit of serving as quantitative global parameters with which to anchor the EIMP CFD simulations to the experimental results. Previously, the anchoring was to be performed simply by the point-to-point comparison of experimental versus computational fuel and pitot pressure contours, which is not as rigorous as a comparison based upon a global metric. More broadly, this work has proven that it is not required to experimentally determine mixing efficiency, which requires measurement of four independent aerothermodynamic variables, to obtain the true fuel/air mixing performance of a specific fuel injection strategy. This enables accurate determination of mixing performance with a reduced and simplified set of measurements. This conclusion has potentially wide-ranging implications for future experimental studies of high-speed fuel injectors. By using the metrics introduced herein, the experimental characterization of an injector's mixing performance can be expedited, and reliance on CFD can be decreased, without sacrificing the accuracy of the conclusions reached. This will allow for many more injector configurations to be tested in a shorter amount of time than has been traditionally possible.

Acknowledgments

The authors would like to thank Prof. Andrew Cutler of George Washington University for sharing the Transverse Jet Facility experimental data found in ref. [13], which proved highly valuable to this work.

References

[1] Kutschenreuter, P., "Supersonic Flow Combustors," *Scramjet Propulsion*, edited by E. T. Curran and S. N. B. Murthy, Progress in Astronautics and Aeronautics, AIAA, Reston, VA, 2000, pp. 513–568.

[2] Seiner, J. M., Dash, S. M., and Kenzakowski, D. C., "Historical Survey on Enhanced Mixing in Scramjet Engines," *9th International Space Planes and Hypersonic Systems and Technologies Conference*, AIAA 99-4869, Norfolk, VA, 1999.

[3] Gutmark, E. J., Schadow, K. C., and Yu, K. H., "Mixing Enhancement in Supersonic Free Shear Flows," *Annual Review of Fluid Mechanics*, Vol. 27, 1995, pp. 375–417. doi:10.1146/annurev.fl.27.010195.002111.

[4] Lee, J., Lin, K., and Eklund, D., "Challenges in Fuel Injection for High-Speed Propulsion Systems," *AIAA Journal*, Vol. 53, No. 6, 2015, pp. 1405–1423. doi:10.2514/1.J053280.

[5] Mao, M., Riggins, D. W., and McClinton, C. R., "Numerical Simulation of Transverse Fuel Injection," *Computational Fluid Dynamics Symposium on Aeropropulsion*, NASA, Cleveland, OH, 1990, pp. 635–667.

[6] Fuller, R. P., Wu, P., Nejad, A. S., and Schetz, J. A., "Comparison of Physical and Aerodynamic Ramps as Fuel Injectors in Supersonic Flow," *Journal of Propulsion and Power*, Vol. 14, No. 2, 1998, pp. 135–145. doi:10.2514/2.5278.

[7] Donohue, J. M., and McDaniel Jr., J. C., "Complete Three-Dimensional Multiparameter Mapping of a Supersonic Ramp Fuel Injector Flowfield," *AIAA Journal*, Vol. 34, No. 3, 1996, pp. 455–462. doi:10.2514/3.13089.

[8] Donohue, J. M., Victor, K. G., and McDaniel Jr., J. C., "Computer-Controlled Multi-Parameter Mapping of 3D Compressible Flowfields Using Planar Laser-Induced Iodine Fluorescence," *31st AIAA Aerospace Sciences Meeting and Exhibit*, AIAA 93-0048, Reno, NV, 1993.

[9] Liscinsky, D. S., True, B., and Holdeman, J. D., "Experimental Investigation of Crossflow Jet Mixing in a Rectangular Duct," *29th AIAA/SAE/ASME/ASEE Joint Propulsion Conference and Exhibit*, AIAA 93-2037, Monterey, CA, 1993.

[10] Doster, J. C., King, P. I., Gruber, M. R., Carter, C. D., Ryan, M. D., and Hsu, K. Y., "In-Stream Hypermixer Fueling Pylons in Supersonic Flow," *Journal of Propulsion and Power*, Vol. 25, No. 4, 2009, pp. 885–901. doi:10.2514/1.40179.

[11] Ground, C. G., Drozda, T. G., Cabell, K. F., and Axdahl, E. L., "Comparison of Several Global Mixing Performance Metrics for High-Speed Fuel Injectors," *22nd AIAA International Space Planes and Hypersonic Systems and Technologies Conference*, AIAA 2018-5261, Orlando, FL, 2018.

[12] Cabell, K., Drozda, T. G., Axdahl, E. L., and Danehy, P. M., "The Enhanced Injection and Mixing Project at NASA Langley," *JANNAF 46th CS / 34th APS / 34th EPSS / 28th PSHS Joint Subcommittee Meeting*, Albuquerque, NM, 2014.

[13] Doerner, S. E., and Cutler, A. D., "Effects of Jet Swirl on Mixing of a Light Gas Jet in a Superonic Airstream," NASA Contractor Report CR-1999-209842, NASA, Hampton, VA, Dec. 1999.

[14] Drozda, T. G., Drummond, J. P., and Baurle, R. A., "CFD Analysis of Mixing Characteristics of Several Fuel Injectors at Hypervelocity Flow Conditions," *52nd AIAA/SAE/ASEE Joint Propulsion Conference*, AIAA 2016-4764, Orlando, FL, 2016.

[15] Drozda, T. G., Baurle, R. A., and Drummond, J. P., "Impact of Flight Enthalpy, Fuel Simulant, and Chemical Reactions on the Mixing Characteristics of Several Injectors at Hypervelocity Flow Conditions," *63rd JANNAF Propulsion Meeting / JANNAF 47th CS / 35th APS / 35th EPSS / 29th PSHS / Joint Subcommittee Meeting*, Newport News, VA, 2016.

[16] Drozda, T. G., Shenoy, R. R., Passe, B. J., Baurle, R. A., and Drummond, J. P., "Comparison of Mixing Characteristics for Several Fuel Injectors on an Open Plate and in a Ducted Flowpath Configuration at Hypervelocity Flow Conditions," *JANNAF 48th CS / 36th APS / 36th EPSS / 30th PSHS / PIB Joint Subcommittee Meeting*, Newport News, VA, 2017.

[17] Drozda, T. G., Cabell, K. F., Ziltz, A. R., Hass, N. E., Inman, J. A., Burns, R. A., Bathel, B. F., Danehy, P. M., Abdul-Huda, Y. M., and Gamba, M., "Comparisons Between NO PLIF Imaging and CFD Simulations of Mixing Flowfields for High-Speed Fuel Injectors," *53rd AIAA/SAE/ASEE Joint Propulsion Conference, AIAA Propulsion and Energy Forum*, AIAA 2017-4647, Atlanta, GA, 2017.

[18] Drozda, T. G., Cabell, K. F., Ziltz, A. R., Hass, N. E., Inman, J. A., Burns, R. A., Bathel, B. F., and Danehy, P. M., "Comparisons Between NO PLIF Imaging and CFD Simulations of Mixing Flowfields for High-Speed Fuel Injectors," *JANNAF 48th CS / 36th APS / 36th EPSS / 30th PSHS / PIB Joint Subcommittee Meeting*, Newport News, VA, 2017.

[19] Baurle, R. A., Fuller, R. P., White, J. A., Chen, T. H., Gruber, M. R., and Nejad, A. S., "An Investigation of Advanced Fuel Injection Schemes for Scramjet Combustion," *36th AIAA Aerospace Sciences Meeting and Exhibit*, 1998.

[20] Ogawa, H., "Physical Insight into Fuel-Air Mixing for Upstream-Fuel-Injected Scramjets via Multi-Objective Design Optimization," *Journal of Propulsion and Power*, Vol. 31, No. 6, 2015, pp. 1505–1523. doi:10.2514/1.B35661.

[21] Guy, R. W., Torrence, M. G., Sabol, A. P., and Mueller, J. N., "Operating Characteristics of the Langley Mach 7 Scramjet Test Facility," Tech. Rep. TM-81929, NASA, 1981.

[22] Thomas, S., and Guy, R., "Expanded Operational Capabilities of the Langley Mach 7 Scramjet Test Facility," Tech. Rep. TP-2186, NASA, 1983.

[23] Guy, R. W., Rogers, R. C., Puster, R. L., Rock, K. E., and Diskin, G. S., "The NASA Langley Scramjet Test Complex," *32nd AIAA, ASME, SAE and ASEE Joint Propulsion Conference*, Lake Buena Vista, FL, 1996.

[24] Brown, G. L., and Rebollo, M. R., "A Small, Fast-Response Probe to Measure Composition of a Binary Gas Mixture," *AIAA Journal*, Vol. 10, No. 5, 1972, pp. 649–652. doi:10.2514/3.50170.

[25] Ninnemann, T. A., and Ng, W. F., "A Concentration Probe for the Study of Mixing in Supersonic Shear Flows," *Experiments in Fluids*, Vol. 13, No. 2-3, 1992, pp. 98–104. doi:10.1007/BF00218155.

[26] Cutler, A. D., and Johnson, C. H., "Analysis of Intermittency and Probe Data in a Supersonic Flow with Injection," *Experiments in Fluids*, Vol. 23, No. 1, 1997, pp. 38–47. doi:10.1007/s003480050084.

[27] Ground, C. R., Viganó, D., and Maddalena, L., "Comparison of Intrusive and Non-Intrusive Mixture Composition Measurements in Supersonic Flow," *Journal of Propulsion and Power*, Vol. 34, No. 6, 2018, pp. 1574–1585. doi:10.2514/1.B36836.

[28] Ground, C. R., Gopal, V., and Maddalena, L., "Filtered Rayleigh Scattering Mixing Measurements of Merging and Non-merging Streamwise Vortex Interactions in Supersonic Flow," *Experiments in Fluids*, Vol. 59, No. 4, 2018, pp. 67–73. doi:10.1007/s00348-018-2521-4.

[29] Waitz, I. A., Marble, F. E., and Zukoski, E. E., "A Systematic Experimental and Computational Investigation of a Class of Contoured Wall Fuel Injectors," *30th AIAA Aerospace Sciences Meeting and Exhibit*, AIAA 92-0625, Reno, NV, 1992.

[30] Buttsworth, D. R., and Jones, T. V., "Concentrattion Probe Measuremens in a Mach 4 Nonreacting Hydrogen Jet," *Journal of Fluids Engineering*, Vol. 125, No. 4, 2003, pp. 628–635. doi:10.1115/1.1595671.

[31] Gruber, M. R., Carter, C. D., Montes, D. R., Haubelt, L. C., King, P. I., and Hsu, K. Y., "Experimental Studies of Pylon-Aided Fuel Injection into a Supersonic Crossflow," *Journal of Propulsion and Power*, Vol. 24, No. 3, 2008, pp. 460–470. doi:10.2514/1.32231.

[32] Arakawa, T., Nojima, K., Kobayashi, K., and Tomioka, S., "Dominant Parameter to Match Fuel/Air Mixing between Reacting and Nonreacting Flows in Dual-mode Combustor," *54th AIAA/SAE/ASEE Joint Propulsion Conference*, AIAA 2018-4931, Cincinatti, Oh, 2018.

[33] McGann, B., Lee, T., Ombrello, T. M., Carter, C. D., Hammack, S. D., and Do, H., "Statistical Measurments of Fuel Mole Fraction in Scramjet Cavity Flameholder with a Fuel Surrogate," *AIAA SciTech 2019 Forum*, 2019.

[34] VULCAN-CFD, "http://vulcan-cfd.larc.nasa.gov/," , Dec. 2017.

[35] Drozda, T. G., Axdahl, E. L., and Cabell, K. F., "Pre-Test CFD for the Design and Execution of the Enhanced Injection and Mixing Project at NASA Langley Research Center," *JANNAF 46th CS / 34th APS / 34th EPSS / 28th PSHS Joint Subcommittee Meeting*, Albuquerque, NM, 2014.